Journal of Ultrafine Grained and Nanostructured Materials
https://jufgnsm.ut.ac.ir
Vol. 54, No.1, June 2021, pp. 73-84
Print ISSN: 2423-6845 Online ISSN: 2423-6837
DOI: 10.22059/jufgnsm.2021.01.08

Function finding via genetic expression programming to predict microhardness of Ni/Al_2O_3 nanocomposite coatings

Mahboubeh Dehestani, Gholam Reza Khayati*, Shahriar Sharafi

Department of Materials Science and Engineering, Shahid Bahonar University of Kerman, Kerman, Iran.

Recieved: 30 March 2020; Accepted: 10 December 2020
** Corresponding author email: khayati@uk.ac.ir*

ABSTRACT

A new proposing model based on gene expression programming (GEP) to predict microhardness of Ni/Al_2O_3 nanocomposite coating was the subject of the present study. Accordingly, a series of the laboratory experiments was designed by the factorial D-optimal array. This was accomplished by considering the most effecting practical electrodeposition parameters including the amount of Al_2O_3 nanoparticles in the bath, current density, temperature, magnetic stirring rate, time of stirring, and plating time as the input and the microhardness of the coating as the output of model. Various performance criteria including determination (R^2) coefficient, the mean absolute error (MAE), and the root relative squared error (RRSE) were utilized to evaluate the developed models. Finally, the model with R^2 = 0.9752, MAE = 0.030 and RRSE = 0.158 was developed as the optimum proposed function. Also, the results of the sensitivity analysis confirmed that the current density was the most effective parameter, while the amount of Al_2O_3 nanoparticles in the bath, plating time, magnetic stirring rate, time of stirring, and temperature had relatively lower effect. In conclusion, the exclusive features of the GEP simulation have been approved to determine Ni/Al_2O_3 nanocomposite coatings microhardness.

Keywords: *Ni/Al_2O_3 nanocomposite; Microhardness; Electrodeposition; Gene expression programming.*

1. Introduction

Recently, there are growing demands to improve of the properties of composite coating especially for surface engineering. Generally, such composite coating contains two phases (viz. matrix and reinforcement), which are combined to enhance their properties [1, 2]. Metal matrix composite (MMC) is one of the most common composites in which the matrix is in the form of pure metal or alloy and the reinforcement is fabricated from ceramic particles, metals or organic compounds [3]. In the case of ceramic particles as the reinforcement, mainly oxides or carbides are considered as the various types of the particles. MMCs have widespread applications in automotive, military and aerospace industries due to their excellent isotropic physicochemical characteristics [4].

There are various approaches to prepare of MMCs, e.g. electrodeposition, vacuum infiltration, powder metallurgy and thermal spray [1, 5]. Electrodeposition, has outstanding advantageous compared to the others such as low practical pressures or temperatures, high ability to dope the inert particles as reinforcement in the metallic matrix during the deposition process. Uniform coating preparation, low operating cost, acceptable efficiency as well as the production rate at industrial scales are feasible [6]. Also, the

electrodeposition technique provides a suitable substrate to improve the nanostructures with completely novel and superior properties respect to the coarse-grained structures [1]. Preparation of nanocomposites by applying the electrodeposition technique has been widely reported [7-9]. In this work, we used Al_2O_3 nanoparticle as reinforcement due to the chemical stability, wear resistance at high temperatures, and high hardness. Ni was used as the metallic matrix. This nanocomposite offers the possibility of enhancement of mechanical and tribological characteristics [8]. This idea has been extensively investigated in other investigations [9-11]. Unfortunately, the chemical composition and properties of the electrodeposited composites cannot be properly predicted, and from the practical parameters are changed in a wide range. Such limitations are the main drawbacks to prepare such nanocomposite by electrodeposition. However, optimizing electrodeposition parameters has a key role to improve the nanocomposite characteristics. In this regard, determination of the optimal combination of practical variables to prepare a compact and uniform nanocomposite has a strategic importance [1].

Applying a soft computing tool such as artificial intelligence to determine of the effect of the practical parameters is an efficient approach [12]. Support vector machine, adaptive neuro-fuzzy inference system, artificial neural networks and gene expression programming (GEP), are the typical strategies to be optimized in the artificial intelligence approach [13]. The advantages of GEP including easy coding, fast computations and easy modeling proposed this strategy as a suitable approach for optimization [14]. GEP was invented by Ferreira [15], which is the evolutionary computing algorithm. GEP processes the evolution to find a suitable function and to determine the effective parameters with acceptable efficiency. Utilizing GEP strategy and the selected data set prepared by the practical experiments, the output can be presented as a function of the input variables in the form of an appropriate mathematical equation [16]. To the best of our knowledge, GEP strategy was successfully applied for a different practical engineering processing [17-22].

According to the literature, there are not any reports on the prediction of the microhardness of Ni/Al_2O_3 nanocomposite coatings prepared by electrodeposition. Accordingly, current study preliminary attempts to express some mathematical equations by applying the GEP strategy to predict microhardness of such coatings. In this regard, six independent practical electrodeposition variables were selected as the input, and the microhardness of the coatings as the output of model. The experimental data set were collected by the factorial D-optimal array and performing 105 various reliable trials. For the first time an equation for Ni/Al_2O_3 nanocomposite microhardness was proposed by the GEP approach. It is believed that the proposed model can be applied to surface engineering.

2. Experimental procedure

$10 \times 10 \times 1$ mm^3 stainless steel plates were used as the cathode. Firstly, the cathode was polished with 100 grit finish, then for 60 seconds floated in 15% HCl, and finally washed with acetone. A $20 \times 100 \times 20$ mm^3 nickel plate was selected as the anode. Both electrodes were positioned in a vertical situation at the distance 3 cm. The α-Al_2O_3 diameters were mainly 30 nm (CRM of china, 99.99% purity). Ni/Al_2O_3 nanocomposite coatings were prepared by using the deposition with a direct current. The chemical composition of the Watts bath is given in Table 1.

To collect the experimental data using the factorial D-optimal array, 105 reliable experiments were conducted by changing six practical parameters (vis., the amount of Al_2O_3 nanoparticles in the bath, current density, temperature, magnetic stirring rate, time of stirring and plating time) at various ranges (Table 2). The ranges of experimental variable selected in this study are based on literatures [23-24].

After the electrodeposition, the surface hardness of Ni/Al_2O_3 nanocomposite coatings was measured using a microhardness tester (Shimadzu) by applying a 50 g load. The surface morphology of nanocomposite coating was investigated by SEM (Cam scan 2300 Mv), and the chemical composition of the prepared coatings was determined by EDS. The structural features of the coatings were studied by XRD (Philips X′pert MPD) and Cu-Kα radiation. The typical XRD spectra of the prepared

Table 1- Solution composition for Ni/Al_2O_3 nanocomposite coatings

Component	Concentration (g/L)
Nickel sulfate ($NiSO_4 \cdot 6H_2O$)	250
Nickel chloride ($NiCl_2 \cdot 6H_2O$)	45
Boric acid (H_3BO_3)	40
Saccharin	5

Table 2- Ranges of microhardness and practical variables through preparing Ni/Al_2O_3 nanocomposite coatings by electrodeposition

Parameters	Range	Standard deviation
Temperature (°C)	20-55	12.69
Current density (A/cm²)	0.01-0.05	0.014
Magnetic stirring rate (rpm)	300-600	113.90
Time of stirring (h)	2-24	7.83
Amount of Al_2O_3 (g/L)	0-90	28.94
Plating time (h)	0.5-1	0.21
Microhardness (HV)	92-1044	221.81

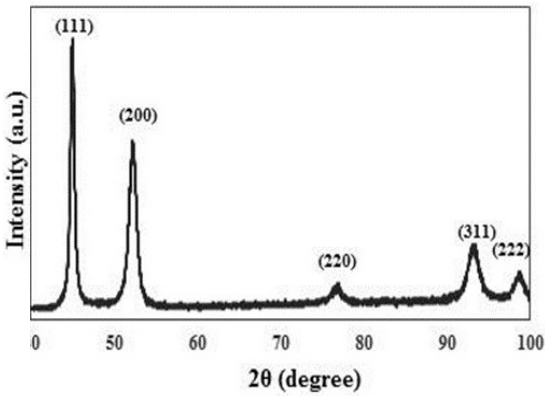

Fig. 1- Typical illustration of the XRD pattern of the Ni/Al_2O_3 nanocomposite coating prepared at the temperature of 45 ˚C, current density of 0.04 A/cm², magnetic stirring rate of 450 rpm, time of stirring of 24 h, with 10 g/L of nano-Al_2O_3 in plating solution and plating time of 1 h.

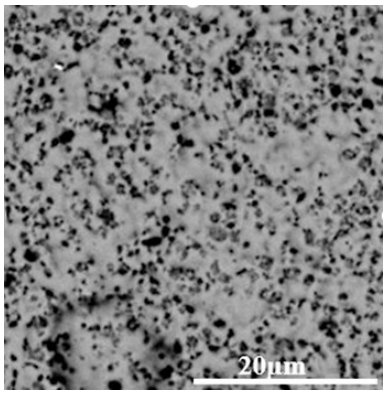

Fig. 2- An example of SEM micrograph of morphology of the surface of Ni/Al_2O_3 nanocomposite coatings prepared at the temperature of 45 °C, current density of 0.04 A/cm², magnetic stirring rate of 450 rpm, time of stirring of 24 h, with 10 g/L of nano-Al_2O_3 in plating solution and plating time of 1 h.

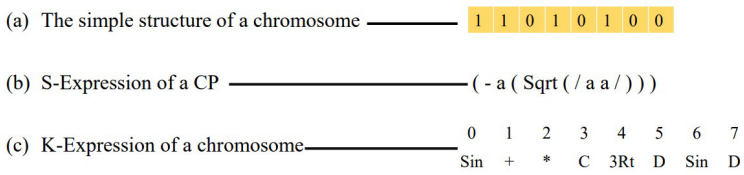

Fig. 3- Comparison between the expression of individuals in (a) GA, (b) GP and (c) GEP.

sample at the temperature of 45 ˚C, current density of 0.04 A/cm², magnetic stirring rate of 450 rpm, time of stirring of 24 h, with 10 g/L of nano-Al_2O_3 in plating solution and plating time of 1 h was shown in Fig. 1. Accordingly, the formation of Ni-based composite coatings on the substrate of steel was confirmed. Also, the mean crystallite size of Ni matrix was found to be of about 22 nm by the Scherrer equation.

The SEM image (with backscatter detector) of this sample illustrates the relatively smooth and compact without any pores or fissures on the surface of the prepared sample (Fig. 2). As observed, the Al_2O_3 nanoparticles (dark spots in SEM image due to their lower average mass unit with respect to the Ni substrate) were distributed homogeneously through the Ni matrix.

3. Model development

GEP is extended version genetic algorithm (GA) and genetic programming (GP). Similar to the GP and GA, GEP has been constructed from random generation of initial populations of chromosomes in the form of solutions and individuals. Moreover, the genetic operators were utilized on the proposed chromosomes and the optimum point was determined. The structure of the individuals is the main difference between in three strategies [25]. As shown in Fig. 3(a), the chromosomes in GAs have binary linear-coded string with a constant length. While, the individuals in GP (Fig. 3(b)) are depicted as computer programs developed based

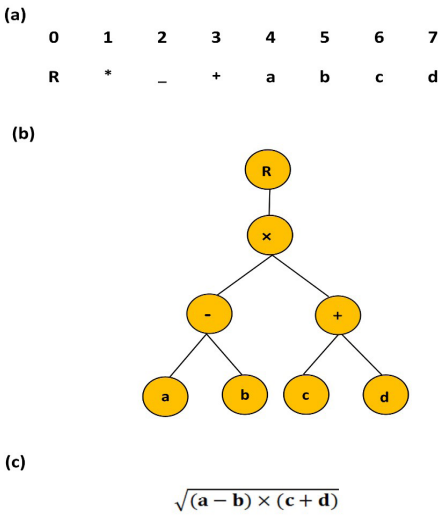

Fig. 4- The structure of simple chromosome with (a) K-Expression, (b) ET and (c) mathematical function.

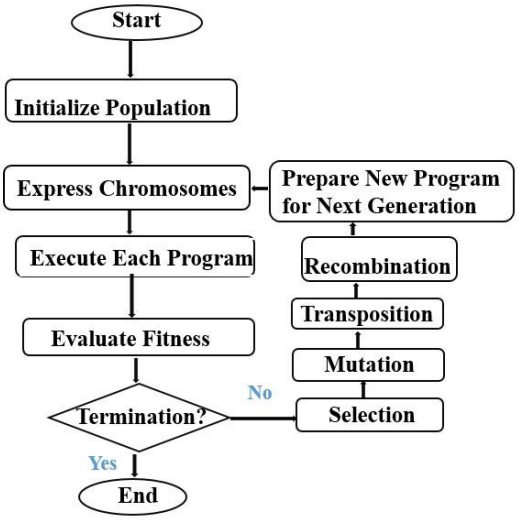

Fig. 5- GEP strategy flowchart.

on LISP language and provide the possibility of representation of their structure as tree structures in various shapes and sizes named a parse trees. In the hybrid strategy of GA and GP, the individuals depicted as linear-coded strings that followed the Karva language proposed by Ferreira [15] for GEP. This language is designed to read and depict the coded programs in the chromosomes (Fig. 3(c)). The possibility of illustration of Karva language in the form of expression trees (Ets) is another advantage of GEP. Accordingly, the GEP strategy is composed of two main parts including the chromosomes and Ets.

There are one or more genes in each chromosome of GEP made of a head and a tail. GEP designer determines the length of the head while the tail length is calculated by following equation [15, 25].

$$t = h(n_{max} - 1) + 1 \quad (1)$$

Where t, h and n_{max} are the length of chromosome head, length of chromosome tail, and number of arguments, respectively. Function sets (such as "+, -, /, *, Sqrt, 3Rt, Sin, Cos, Tan, Arctan, Ln, Exp"), and logic function (such as and, or) with terminals (model input) are the components of each linear strings. The schematic of the process of GEP is shown in Fig. 4. Accordingly, at first, an initial population of chromosomes as a random way is produced. Then, these chromosomes are encoded as Fig. 4 (a) or depicted as ET in Fig. 4 (b). Finally, in the Fig. 4 (c), the mathematical function of the proposed ETs was extracted. The fitting parameters of each model were estimated by applying the fitness function.

In order to satisfy the number of generation or the best solution, the modeling process will be continued. If the process doesn't stop, genetic operators are applied. In this regard, the generation with a better chromosome will be selected by means of try and error with considering its fitness as a criteria and it is replicated into the next generation. Then, the mutation operator was utilized in a way that the length of chromosome is kept constant. This operator is able to perform in both sections of chromosome. As an example, mutation is able to change any terminal with a function or together in the head. This operator can just replace the terminal with the other terminal in the tail. The rate of mutation (between 0.01 and 0.1) can be occurred in the length of chromosome. Insertion sequence is the other operator in GEP which can be applied to the chromosome and provides the movement of the fragment. Crossover or recombination operators utilized on the chromosome, providing the possibility of changing the fragments between two selected chromosomes. One-point, two-point and gene recombination are the three types of recombination. When these three genetic operators are applied, the second generation is generated and this process is kept on to meet the termination criteria [15,

Table 3- Parameters of GEP models

Code	Parameter	Settings			
		1	2	3	4
P1	Number of chromosomes	30	35	40	-
P2	Head size	9	10	11	-
P3	Number of genes	3	4	5	6
P4	Linking function	Addition (+), Multiplication (*)			
P5	Fitness function error type	RRSE			
P6	Constant per gene	1			
P7	Mutation rate	0.00138			
P8	Inversion rate	0.00546			
P9	One-point recombination rate	0.00277			
P10	Two-point recombination rate	0.00277			
P11	Gene recombination rate	0.00277			

Table 4- List of function sets

Code	Function set
S1	+, *, /, -, Exp, Ln, Sqrt,3Rt, Atan,x^2, x^3
S2	+, *, /, -, Exp, Ln, x^2, x^3, x^4, x^5, Sqrt, 3Rt, 4Rt, 5Rt
S3	+, *, /, -, Sqrt, 3Rt,x^2, x^3, Sin, Cos, Sec
S4	+, *, /, -, x^2, x^3,Sin, Cos, Asin, Acos
S5	+, *, /, -, , Ln, Exp, x^2, Sin, Cos, Atan, tanh
S6	+, *, /, -, Exp, Ln, Sqrt, x^2, x^3, 3Rt, 4Rt, Sin, Cos

25, 27, 28]. Fig. 5 is illustrated the GEP flowchart.

The most appropriate solution of GEP strategy is obtained, when one or more genetic chromosomes have been used. Each chromosome is considered as sub-ET, and by linking of all sub-ET will prepare the complex ET. There are various linking functions including addition and multiplication that are the most common types.

In this context, for the first time an important branch of artificial intelligence named GEP was utilized to model the microhardness of Ni/Al_2O_3 nanocomposites. In this regard, 105 microhardness measurements were made. The practical data was randomly divided into 2 parts (training and testing). Two separate sets introduced to the GEP models. Testing data (including 30 datasets) is randomly chosen from the total data to generalize the model while the rest is the training data which is used to train the model. This ensures that if the regression of the testing data was high, the regression got from the training data is not false. This action increases the model accuracy several times. Before training the GEP model, each parameter has been normalized to a certain range of (0, 1).

To validate the models and select the most appropriate one, various statistical criteria were utilized. The mean absolute error (MAE), root relative squared error (RRSE) and coefficient of determination (R^2) are the most common of these criteria. R^2 was employed to determine the compatibility of the predicted data compared to the experimental ones. Their values are obtained from the following equations:

$$MAE = \frac{1}{n}\left[\frac{\sum_{i=1}^{n}|t_i - p_i|}{\sum_{i=1}^{n} t_i}\right] \quad (2)$$

$$RRSE = \sqrt{\frac{\sum_{i=1}^{n}(t_i - p_i)^2}{\sum_{i=1}^{n}(t_i - \bar{t}_i)^2}} \quad (3)$$

$$R^2 = 1 - \frac{\sum_{i=1}^{n}(t_i - p_i)^2}{\sum_{i=1}^{n}(t_i - \bar{t}_i)^2} \quad (4)$$

Where p_i is predicted microhardness, t_i, $\bar{t}_i$ and n are actual microhardness, average of microhardness during two runs of measurement, and number of samples, respectively.

4. Results and discussion

Various configurations of GEP models with various parameters including chromosomes number, length of head, genes number and linking function are investigated. Among them, only models with the higher accuracy were selected as candidate for further analysis. Selected parameters and the list of function sets of the investigated GEP models are abbreviated in Tables 3 and 4.

The performance of each GEP model was

Table 5- Comparison of R^2, MAE and RRSE for the best GEP models

No.	P1	P2	P3	P4	Function set	Training			Testing		
						R^2	MAE	RRSE	R^2	MAE	RRSE
GEP 1	3	1	2	*	S2	0.9752	0.030	0.158	0.9894	0.017	0.122
GEP 2	1	1	3	+	S3	0.8921	0.132	0.349	0.9082	0.086	0.307
GEP 3	2	1	4	+	S6	0.9351	0.114	0.260	0.9418	0.081	0.273
GEP 4	3	2	3	*	S5	0.9178	0.124	0.307	0.9196	0.087	0.319
GEP 5	1	3	2	+	S1	0.9068	0.128	0.329	0.8985	0.099	0.403
GEP 6	2	2	3	*	S4	0.9556	0.107	0.229	0.9715	0.064	0.174

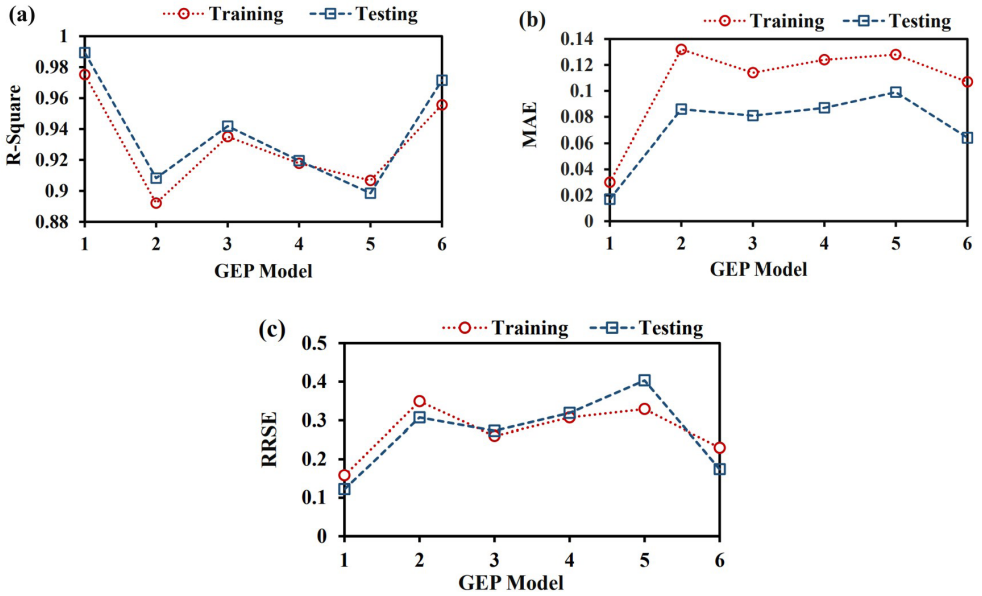

Fig. 6- The variation of (a) R-Square, (b) MAE, and (c) RRSE versus the validated GEP models.

investigated in terms of the statistical indices viz. R^2, MAE, RRSE. In this regard, closer R^2 values to 1 and error indices to zero are the sign of the higher precision. Table 5 summarizes the compared values of the statistical indices for 6 GEP models.

The comparison of the validated GEP models criteria R^2, MAE and RRSE values to train and to test the datasets are shown in Fig. 6. Based on Fig. 6 (a), GEP 1, GEP 6, GEP 3, GEP 4, GEP 5 and GEP 2 have R^2 values closer to 1 during the training mode, respectively. While this rank in the testing mode are as GEP 1, GEP 6, GEP 3, GEP 4, GEP 2 and GEP 5, respectively. As a consequence, from R^2 values, all 6 GEP models have an acceptable accuracy to predict microhardness of Ni/Al_2O_3 nanocomposite coating. However, GEP 1 is preferable to the others. By consideration of RRSE as the criteria to validate the performance, GEP 1 with the RRSE equals to 0.158 and 0.122 have the lowest values in training and testing mode.

Before choosing GEP 1 as the most appropriate model in Table 5, examination of GEP setting parameters effect on the performances of GEP 1 would be significantly beneficial. In this regards, the selection of optimum setting parameters (i.e., number of chromosomes, number of gene, linking function and gene head size) plays a key role in the performance of GEP models. Accordingly, to investigate the effect of the setting parameters on the performance of GEP 1 model (as the best proposed model), the number of chromosomes, head size, genes number in two modes of linking function viz., multiplication and addition have been changed. It was necessary to note that, the selection of suitable values during the setting is a function of the number of possible solution as well as complexity of the problem. A number of chromosomes in two modes of the linking function viz., multiplication and addition were changed in GEP 1. Table 6 summarized various changes in GEP 1 configuration to investigate the possibility through improving of its performance.

Table 6- Change in number of chromosomes for GEP 1 model upon criteria R^2, MAE and RRSE in multiplication and addition mode

No.	P1	P2	P3	P4	Training			Testing		
					R^2	MAE	RRSE	R^2	MAE	RRSE
GEP 1-1	1	1	2	*	0.8948	0.131	0.346	0.9367	0.085	0.300
GEP 1-2	2	1	2	*	0.9037	0.132	0.351	0.9292	0.084	0.298
GEP 1-3	3	1	2	*	0.9752	0.030	0.158	0.9894	0.017	0.122
GEP 1-4	1	1	2	+	0.9314	0.130	0.3371	0.9390	0.085	0.299
GEP 1-5	2	1	2	+	0.9258	0.126	0.3186	0.9686	0.071	0.212
GEP 1-6	3	1	2	+	0.9074	0.131	0.3436	0.9508	0.083	0.291

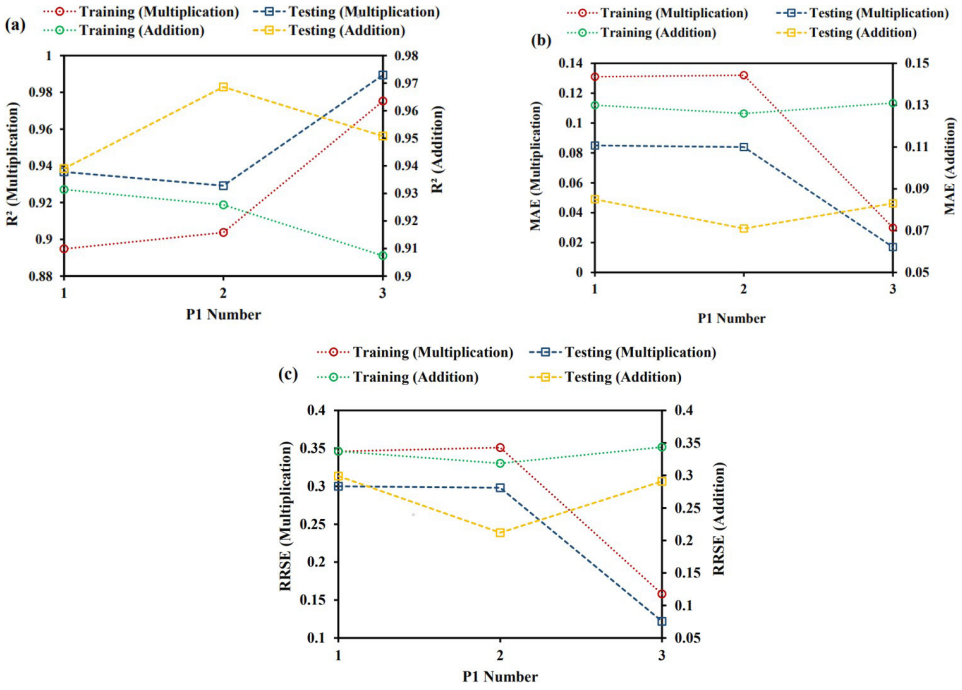

Fig. 7- The variation of (a) R^2, (b) MAE, and (c) RRSE in multiplication and addition mode versus number of chromosomes for GEP 1.

Fig. 7 shows the values of R^2, MAE and RRSE indices at different chromosome number of GEP 1. As observed, the best value of R^2 (closer to 1) and MAE, RRSE (closer to zero) belong to the chromosome number 40 (P1=3) with linking function of multiplication. There is a direct dependency between the complexity of variables and the head size of GEP model evolutions. In other words, higher head size number or higher nodes size in ETs corresponds to the higher complexity of GEP models [15]. To obtain the optimum head size in current study, the head size of GEP 1 changed in two modes of linking function including multiplication and addition.

Based on the performance strategy discussed above (i.e. the models with higher R^2 and lower errors as well as smaller head size), it can be concluded that GEP 1/1 with multiplication mode in Table 7 and Fig. 8 has the best performance with the proposed models. From this, a simple function for microhardness of Ni/Al_2O_3 nanocomposites could be derived when the head size is chosen as small within the size range.

At the next step, the changes in genes number were investigated. According to the Ferreira [15], the enhanced number of the genes from one to three would considerably increase the success rate. It was observed that more than 4 genes did not have any effect on GEP model performance [14]. Hence, the effects of genes number have been investigated by changing its value from 1 to 4 on the best proposed model (GEP 1).

Based on Table 8 and Fig. 9, GEP 1(2) model with head size 4 (P3=2) shows the best performances. Accordingly, by variation of effective parameter through the GEP settings (viz.,

Table 7- Changes in head size for GEP 1 model upon criteria R2, MAE and RRSE in multiplication and addition mode

No.	P1	P2	P3	P4	Training			Testing		
					R^2	MAE	RRSE	R^2	MAE	RRSE
GEP 1/1	3	1	2	*	0.9752	0.030	0.158	0.9894	0.017	0.122
GEP 1/2	3	2	2	*	0.8839	0.135	0.367	0.9067	0.091	0.348
GEP 1/3	3	3	2	*	0.9098	0.130	0.334	0.9533	0.078	0.254
GEP 1/4	3	1	2	+	0.9175	0.134	0.362	0.9695	0.087	0.320
GEP 1/5	3	2	2	+	0.9414	0.113	0.255	0.9752	0.064	0.174
GEP 1/6	3	3	2	+	0.9305	0.125	0.314	0.9374	0.082	0.284

Table 8- Changes in genes number for GEP 1 model upon criteria R^2, MAE and RRSE in multiplication and addition

No.	P1	P2	P3	P4	Training			Testing		
					R^2	MAE	RRSE	R^2	MAE	RRSE
GEP 1(1)	3	1	1	*	0.9023	0.129	0.333	0.9409	0.080	0.269
GEP 1(2)	3	1	2	*	0.9752	0.030	0.158	0.9894	0.017	0.122
GEP 1(3)	3	1	3	*	0.9228	0.122	0.297	0.9543	0.075	0.234
GEP 1(4)	3	1	4	*	0.8930	0.130	0.337	0.8516	0.100	0.419
GEP 1(5)	3	1	1	+	0.9328	0.115	0.264	0.9261	0.085	0.303
GEP 1(6)	3	1	2	+	0.8539	0.138	0.382	0.8515	0.103	0.440
GEP 1(7)	3	1	3	+	0.9252	0.138	0.382	0.9372	0.091	0.343
GEP 1(8)	3	1	4	+	0.9455	0.113	0.255	0.9396	0.083	0.287

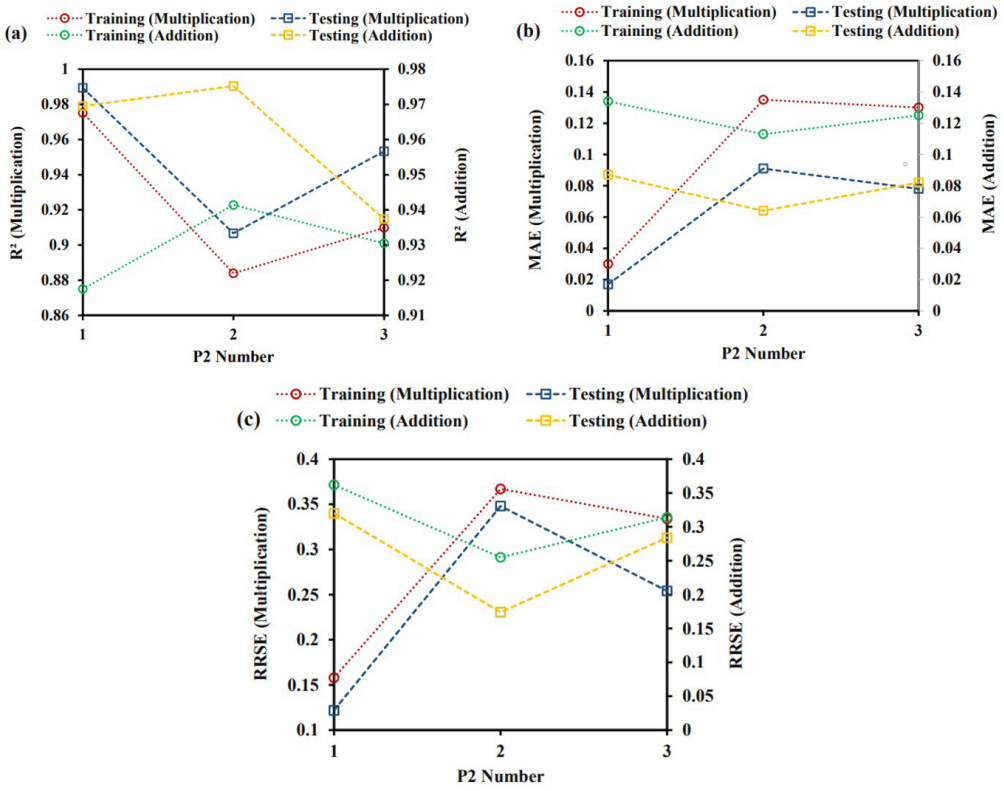

Fig. 8- The variation of (a) R^2, (b) MAE, and (c) RRSE in multiplication and addition mode versus Head size for GEP 1.

number of chromosomes, head size and number of genes) provide the possibility of determination of the optimal configurations. As shown, there are not a regular and consistent trend through changing in GEP settings and performance criteria (i.e., error and R^2). Consequently, GEP 1 with chromosomes number of 40 head size 9 and genes number 4 with multiplication as linking function satisfied

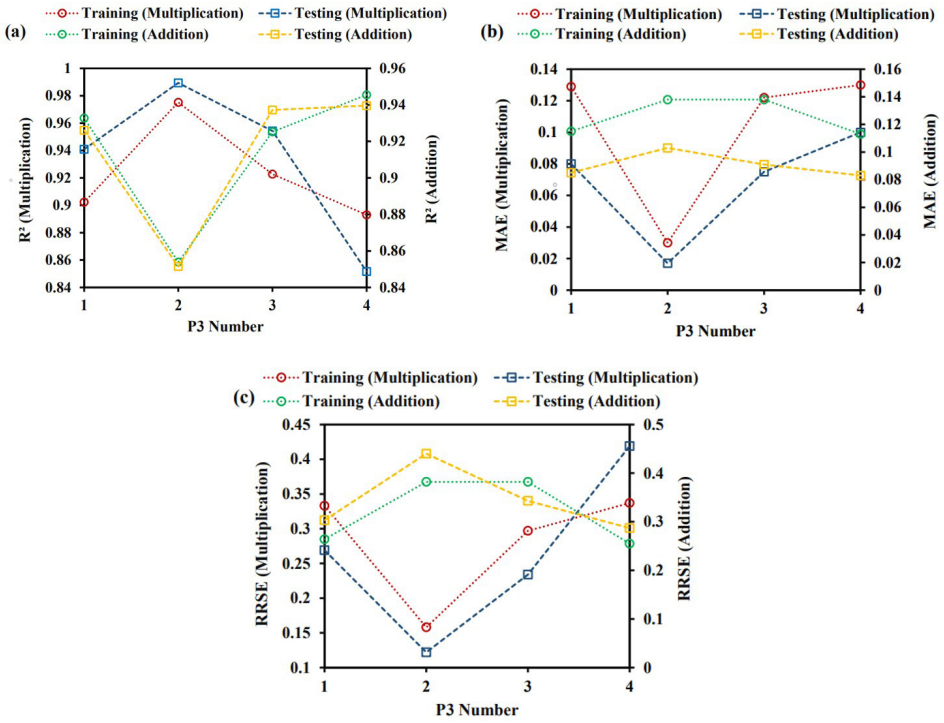

Fig. 9- The variation of (a) R^2, (b) MAE, and (c) RRSE in multiplication and addition mode versus genes number for GEP 1.

Table 9- Representation of the most appropriate model estimated from GEP-1 approaches

Mathematical formulation
Microhardness=Sub − ET1 × Sub − ET2 × Sub − ET3 × Sub − ET4
Sub- ET1 $=\left(\sqrt[4]{\sqrt[3]{\left(\exp\left(\left(\frac{d_2}{-0.548}\right)+\left(\frac{d_1}{-0.548}\right)\right)\times\exp\left(\sqrt[5]{(-0.548)-d_2}\right)\right)}}\right)^2$
Sub- ET2$=\sqrt[5]{\left(\sqrt[5]{\left(\sqrt[4]{6.423}\times(6.423+d_5)\right)}+\left(\sqrt[3]{{d_0}^4}+\sqrt{d_3}\right)\right)^2}$
Sub- ET3$=\left(\left(\sqrt[5]{d_4\times d_1}\right)-\left(\sqrt[5]{d_1}\times 0.497\right)\right)\times\sqrt[5]{\sqrt[3]{d_2}}^3+0.497$
Sub ET4$=\left(\sqrt[4]{d_4\times\sqrt[5]{\left((d_0\times(-0.880))^5+\left(\frac{-0.88}{-0.88}\right)\right)}}\right)^5+d_3$
Note: d_0- Normalized amount of Al_2O_3 (g/L), d_1- Normalized current density (A/cm^2), d_2- Normalized temperature (^0C), d_3- Normalized magnetic stirring rate (rpm), d_4- Normalized time of stirring (h), d_5- Normalized plating time (h).

the predictions with a better accuracy through the training and testing data. The mathematical functions of the microhardness of Ni/Al_2O_3 nanocomposite coating as a function of practical variables derived from proposed GEP model and expressed in Table 9. The ETs of optimum proposed model for the prediction of microhardness are displayed in Fig. 10. As shown, this model including of 4 sub-ETs with the linking function of multiplication.

To provide a deeper explanation from the prediction capability of the proposed GEP model, the predicted values of the GEP 1 based on proposed formulas (Table 9) are graphically compared with the experimental measured values through the training and testing phases. Fig. 11 confirmed that the predicted values reasonably are in agreement with the measured values at the training and testing data. The prediction is well matched with the measured data and this caused an increase in the generalization performance and provides the model prediction with a higher quality.

There is a strong dependency between the quality of the prepared coatings and electrochemical

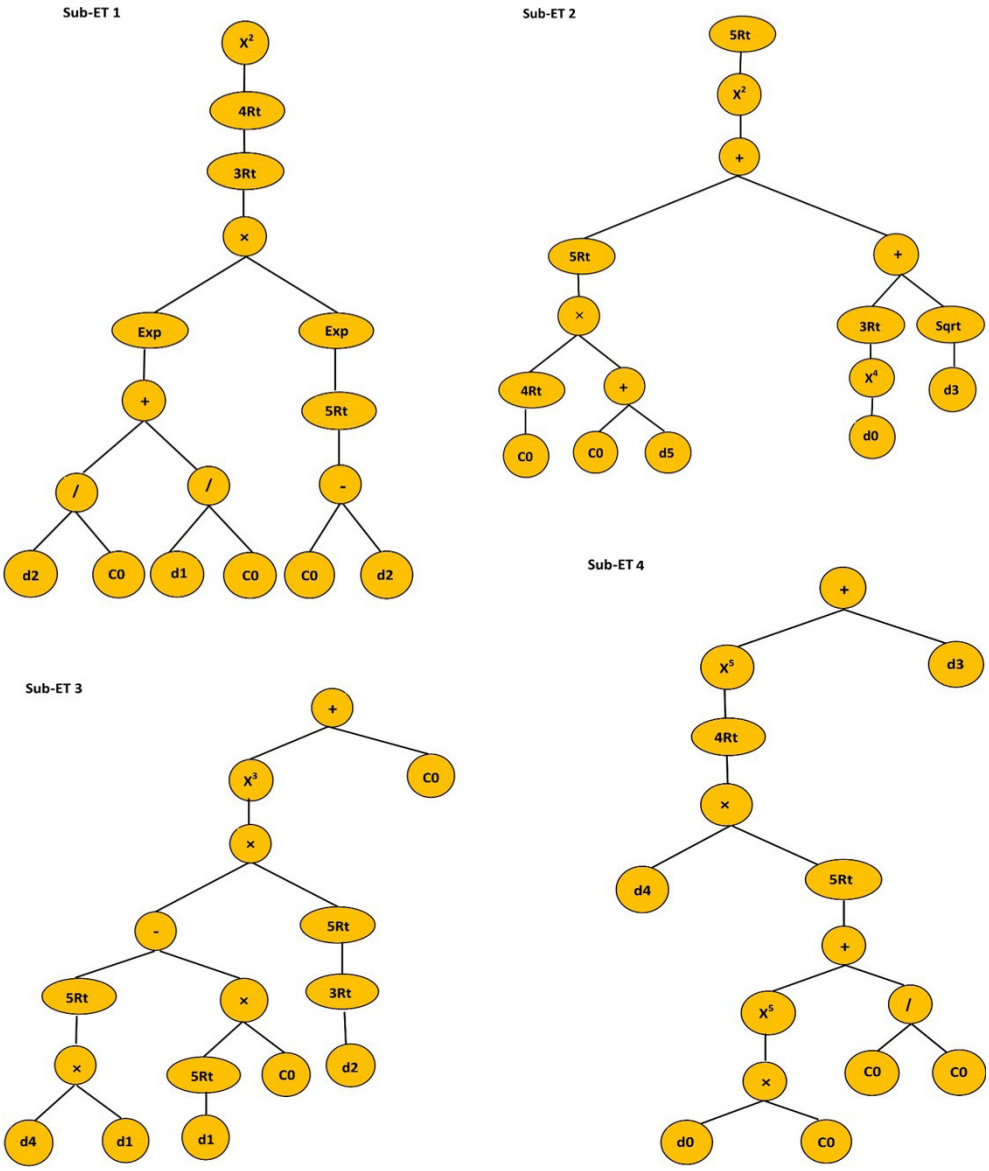

Fig. 10- Expression tree (ET) of the GEP-1 model. (Sub- ET1 C0=-0.548 Sub- ET2 C0=6.422, Sub- ET3 C0=0.497 and Sub- ET4 C0=-0.880).

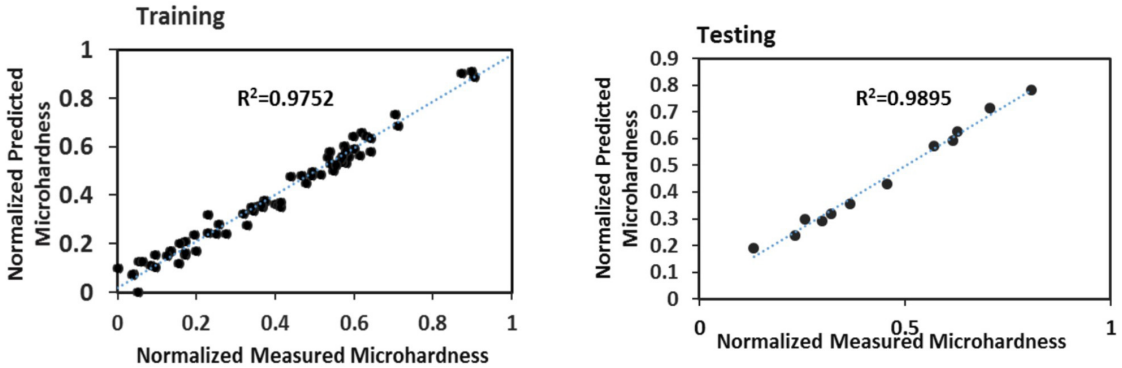

Fig. 11- Measured and predicted microhardness to train and test datasets by using GEP 1 model.

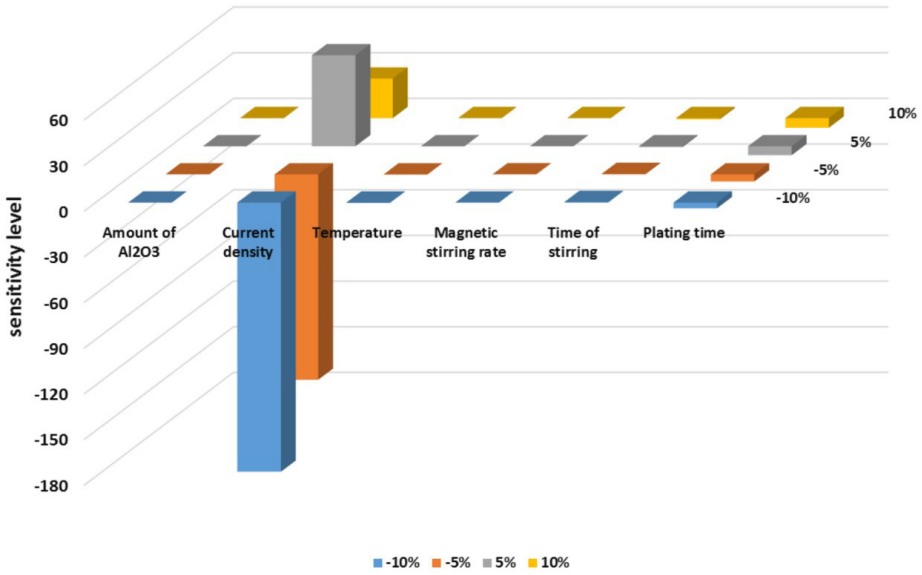

Fig. 12- Sensitivity analysis of practical parameter.

deposition parameter during the preparation of composite coating [23]. Sensitivity analysis has been employed to determine such dependency. As illustrated, current density is the most important one having a significant potential influence on the amount of Al_2O_3 of the prepared composite coating and consequently its microhardness [9]. Such a strong dependency between the microstructure and morphology of the electrodeposited composite coatings has been reported in the literature [23]. Goral [29] showed that any increment in current density enhanced the coating microhardness and due to the higher content of ceramic particles incorporated in the Ni matrix. Also, homogeneous distribution of the ceramic particles was found to be enhanced. It was necessary to note that there is a threshold for direct dependency between the current density and microhardness of prepared composites. As shown in Fig. 12, when the current density beyond from this threshold, does not have the positive effect on the microhardness of the prepared samples.

5. Summary

To predict microhardness of Ni/Al_2O_3 nanocomposite that prepared by electrochemical deposition, gene expression programming (GEP) is employed as a promising evolutionary algorithm to construct a reliable model in this study. Optimization of the best GEP model has been continued by changes in the effective GEP parameters, viz., the chromosomal architecture (the head length, chromosomes and genes numbers), and the type of linking function. To conclude, the GEP structure with 4 genes, 9 head size and 40 chromosomes is proposed as the most appropriate training modeling strategy. The values of R^2, MAE and RRSE related to the optimized GEP model were estimated to be about 0.9752, 0.030 and 0.158, respectively. Also, the sensitivity analysis illustrated that in our investigated regions, current density was the most dominant parameter on the microhardness of the prepared samples.

References

1. Beltowska-Lehman E, Bigos A, Indyka P, Chojnacka A, Drewienkiewicz A, Zimowski S, et al. Optimisation of the electrodeposition process of Ni-W/ZrO 2 nanocomposites. Journal of Electroanalytical Chemistry. 2018;813:39-51.
2. Gurrappa I, Binder L. Electrodeposition of nanostructured coatings and their characterization-A review. Sci Technol Adv Mater. 2008;9(4):043001-.
3. Casati R, Vedani M. Metal Matrix Composites Reinforced by Nano-Particles—A Review. Metals. 2014;4(1):65-83.
4. Ibrahim IA, Mohamed FA, Lavernia EJ. Particulate reinforced metal matrix composites — a review. Journal of Materials Science. 1991;26(5):1137-56.
5. Grewal HS, Agrawal A, Singh H, Shollock BA. Slurry Erosion Performance of Ni-Al2O3 Based Thermal-Sprayed Coatings: Effect of Angle of Impingement. Journal of Thermal Spray Technology. 2013;23(3):389-401.
6. Jiang SW, Yang L, Pang JN, Lin H, Wang ZQ. Electrodeposition of Ni-Al2O3 composite coatings with combined addition of SDS and HPB surfactants. Surface and Coatings Technology. 2016;286:197-205.
7. Benea L, Danaila E, Celis J-P. Influence of electro-co-deposition parameters on nano-TiO2 inclusion into nickel matrix and properties characterization of nanocomposite coatings obtained. Materials Science and Engineering: A. 2014;610:106-15.

8. Góral A. Nanoscale structural defects in electrodeposited Ni/Al 2 O 3 composite coatings. Surface and Coatings Technology. 2017;319:23-32.
9. Lajevardi SA, Shahrabi T, Szpunar JA. Synthesis of functionally graded nano Al2O3–Ni composite coating by pulse electrodeposition. Applied Surface Science. 2013;279:180-8.
10. Gül H, Kılıç F, Aslan S, Alp A, Akbulut H. Characteristics of electro-co-deposited Ni–Al2O3 nano-particle reinforced metal matrix composite (MMC) coatings. Wear. 2009;267(5-8):976-90.
11. Borkar T, Harimkar SP. Effect of electrodeposition conditions and reinforcement content on microstructure and tribological properties of nickel composite coatings. Surface and Coatings Technology. 2011;205(17-18):4124-34.
12. Coşkun Mİ, Karahan İH. Modeling corrosion performance of the hydroxyapatite coated CoCrMo biomaterial alloys. Journal of Alloys and Compounds. 2018;745:840-8.
13. Mehdizadeh S, Behmanesh J, Khalili K. Application of gene expression programming to predict daily dew point temperature. Applied Thermal Engineering. 2017;112:1097-107.
14. Muzzammil M, Alama J, Danish M. Scour Prediction at Bridge Piers in Cohesive Bed Using Gene Expression Programming. Aquatic Procedia. 2015;4:789-96.
15. Ferreira C. The Basic Gene Expression Algorithm. Gene Expression Programming: Springer Berlin Heidelberg. p. 55-120.
16. Güllü H. Function finding via genetic expression programming for strength and elastic properties of clay treated with bottom ash. Engineering Applications of Artificial Intelligence. 2014;35:143-57.
17. Ebrahimzade H, Khayati GR, Schaffie M. A novel predictive model for estimation of cobalt leaching from waste Li-ion batteries: Application of genetic programming for design. Journal of Environmental Chemical Engineering. 2018;6(4):3999-4007.
18. Abdellahi M, Bahmanpour H, Bahmanpour M. The best conditions for minimizing the synthesis time of nanocomposites during high energy ball milling: Modeling and optimizing. Ceramics International. 2014;40(7):9675-92.
19. Ebrahimi-Kahrizsangi R, Abdellahi M, Bahmanpour M. Ignition time of nanopowders during milling: A novel simulation. Powder Technology. 2015;272:224-34.
20. Mahdavi Jafari M, Khayati GR. Prediction of hydroxyapatite crystallite size prepared by sol–gel route: gene expression programming approach. Journal of Sol-Gel Science and Technology. 2018;86(1):112-25.
21. Mansouri I, Chacón R, Hu JW. Improved predictive model to the cross-sectional resistance of CFT. Journal of Mechanical Science and Technology. 2017;31(8):3887-95.
22. Mansouri I, Hu J, Kisi O. Novel Predictive Model of the Debonding Strength for Masonry Members Retrofitted with FRP. Applied Sciences. 2016;6(11):337.
23. Saha RK, Khan TI. Effect of applied current on the electrodeposited Ni–Al2O3 composite coatings. Surface and Coatings Technology. 2010;205(3):890-5.
24. García-Lecina E, García-Urrutia I, Díez JA, Morgiel J, Indyka P. A comparative study of the effect of mechanical and ultrasound agitation on the properties of electrodeposited Ni/Al2O3 nanocomposite coatings. Surface and Coatings Technology. 2012;206(11-12):2998-3005.
25. Khandelwal M, Armaghani DJ, Faradonbeh RS, Ranjith PG, Ghoraba S. A new model based on gene expression programming to estimate air flow in a single rock joint. Environmental Earth Sciences. 2016;75(9).
26. Baykasoglu A, Gullu H, Canakci H, Ozbakir L. Prediction of compressive and tensile strength of limestone via genetic programming. Expert Systems with Applications. 2008;35(1-2):111-23.
27. Ferreira C, Gepsoft, U. What is gene expression programming; 2008.
28. Mollahasani A, Alavi AH, Gandomi AH. Empirical modeling of plate load test moduli of soil via gene expression programming. Computers and Geotechnics. 2011;38(2):281-6.
29. Góral A, Nowak M, Berent K, Kania B. Influence of current density on microstructure and properties of electrodeposited nickel-alumina composite coatings. Journal of Alloys and Compounds. 2014;615:S406-S10.